Freezeout systematics due to the hadron spectrum

Sandeep Chatterjee*
AGH University of Science and Technology, Faculty of Physics and Applied Computer Science, al. Mickiewicza 30, 30-059 Krakow, Poland

Debadeepti Mishra,† Bedangadas Mohanty,‡ and Subhasis Samanta§
School of Physical Sciences, National Institute of Science Education and Research, HBNI, Jatni 752050, India
(Received 14 September 2017; published 15 November 2017)

We investigate systematics of the freezeout surface in heavy ion collisions due to the hadron spectrum. The role of suspected resonance states that are yet to be confirmed experimentally in identifying the freezeout surface has been investigated. We have studied two different freezeout schemes: a unified freezeout scheme where all hadrons are assumed to freeze out at the same thermal state and a flavor-dependent sequential freezeout scheme with different freezeout thermal states for hadrons with or without valence strange quarks. The data of mean hadron yields as well as scaled variance of net proton and net charge distributions have been analyzed. We find the freezeout temperature T to drop by $\sim$5% while the dimensionless freezeout parameters μ_B/T and VT^3 (μ_B and V are the baryon chemical potential and the volume at freezeout respectively) are insensitive to the systematics of the input hadron spectrum. The observed hint of flavor hierarchy in T and VT^3 with only confirmed resonances survives the systematics of the hadron spectrum. It is more prominent in the range $\sqrt{s_{NN}} \sim$ 10–100 GeV, where the maximum hierarchy in T is $\sim$10% and in VT^3 is $\sim$40%. However, the uncertainties in the thermal parameters due to the systematics of the hadron spectrum and their decay properties do not allow us to make a quantitative estimate of the flavor hierarchy yet.

DOI: 10.1103/PhysRevC.96.054907

I. INTRODUCTION

The determination of the last surface of inelastic scattering, the chemical freezeout surface (CFO), is an integral part of the standard model of heavy ion collisions [1–4]. An ideal gas of all the confirmed hadrons and resonances as listed by the Particle Data Group (PDG) [5] forms the hadron resonance gas (HRG) model that has met with considerable success across a broad range of beam energies in describing the mean hadron yields [1–4,6–8] and more recently moments of conserved charges of QCD such as baryon number (B), strangeness (S), and charge (Q) [9–12] with a few thermal parameters. Such an analysis gives us access to the thermodynamic state of the fireball just prior to freezeout. The ongoing hunt for the QCD critical point crucially depends on our knowledge of the background dominated by the thermal hadronic physics close to freezeout.

The HRG partition function $Z(T,\mu_{B,Q,S})$ for a thermal state at (T,μ_B,μ_Q,μ_S), where T is the temperature and μ_B, μ_Q, and μ_S are the chemical potentials corresponding to the three conserved charges B, Q, and S, respectively, can be written as

$$\ln Z = \sum_i \ln Z_i(T,\mu_{B,Q,S}), \tag{1}$$

where Z_i is the single-particle partition function corresponding to the ith hadron species written as

$$\ln Z_i(T,\mu_{B,Q,S}) = VT^3 \frac{a g_i}{2\pi^2} \int dp\, p^2/T^3 \times \ln\left(1 + a e^{-(\sqrt{(p^2+m_i^2)}+\mu_i)/T}\right), \tag{2}$$

where $a = -1$ ($+1$) for mesons (baryons), g_i and m_i refer to the degeneracy factor and mass of the ith hadron species, and μ_i is its hadron chemical potential which, within a complete chemical equilibrium scenario, is written as

$$\mu_i = B_i\mu_B + Q_i\mu_Q + S_i\mu_S, \tag{3}$$

where B_i, Q_i, and S_i are the baryon number, charge, and strangeness of the ith hadron species.

The sum in Eq. (1) runs over all the established resonances from the PDG. However, quark models [13,14] and studies on the lattice [15] predict many more resonances than have been confirmed so far in experiments. It has been pointed out in studies based on comparison between QCD thermodynamics on the lattice and HRG that these resonances could have significant contributions to several thermodynamic quantities [16,17] and influence the extraction of the freezeout parameters within the HRG framework [16]. There have been interesting studies on the status and influence of the systematics of the hadron spectrum on several quantities [18–25]. In this work, we have studied the systematics in the determination of the freezeout surface within the HRG framework due to the uncertainties over the hadron spectrum.

II. EXTRACTING THE CHEMICAL FREEZEOUT SURFACE

The standard practice has been to extract the CFO parameters by fitting the mean hadron yields. The primary yields N_i^p are obtained from Eq. (1) as

$$N_i^p = \frac{\partial}{\partial \mu_i} \ln Z, \tag{4}$$

while the total yields of the stable hadrons that are fitted to data are obtained after adding the secondary contribution from

*Sandeep.Chatterjee@fis.agh.edu.pl
†debadeepti.m@niser.ac.in
‡bedanga@niser.ac.in
§subhasis@niser.ac.in

the resonance decays to their primary yields,

$$N_i^t = N_i^p + \sum_j \mathrm{BR}_{j\to i} N_j^p, \tag{5}$$

where $\mathrm{BR}_{j\to i}$ refers to the branching ratio (BR) of the decay of the jth to ith hadron species.

In this work we characterize the freezeout surface by three parameters, of which only T has dimension. The other two are suitably scaled dimensionless parameters μ_B/T and VT^3. While μ_B/T controls the baryon fugacity factor, VT^3 can be interpreted as the effective phase space volume occupied by the HRG at freezeout. The masses of the hadrons are the relevant scales in this problem. They determine the freezeout T. Thus, it is natural that systematic variation of the hadron spectrum will result in corresponding variation of the freezeout T. On the other hand, the influence of the systematics of the hadron spectrum on the dimensionless parameters μ_B/T and VT^3 is expected to be lesser. This motivates us to work with $(T,\mu_B/T,VT^3)$ instead of the standard choice of (T,μ_B,V). The other parameter that is often used in literature, the strangeness undersaturation factor γ_S, has been taken to be unity here. μ_S and μ_Q are solved consistently from the strangeness neutrality condition and by requiring that the ratio of net B to Q be equal to that of the colliding nuclei (this ratio is ~2.5 for Au and Pb nuclei which we consider here):

$$\text{Net } S = 0, \tag{6}$$

$$\text{Net } B/\text{Net } Q = 2.5. \tag{7}$$

As is evident from Eq. (5), knowledge of the BRs is essential to compute the contribution of the secondary yield, which is the feeddown from the heavier unstable resonances to the observed hadrons. As a result, extraction of the freezeout surface based on the hadron yield data suffers from systematic uncertainties of the decay properties of these additional resonances.

The freezeout surface can also be estimated by comparing higher moments of the conserved charges in experiment and theory [9–12,26–29]. One of the important advantage in using the fluctuations of conserved charges over hadron yields in estimating the freezeout surface is that it is enough to know only the quantum numbers of these unconfirmed states. Decays under strong interactions should conserve the charges B, Q, and S. Thus the conserved charge susceptibilities are not influenced by the systematic uncertainties of the BRs of the unconfirmed resonances.

On the theoretical side, it is straightforward to compute the conserved charge susceptibilities χ^{ijk}_{BQS} of order $(i+j+k)$ from the partition function

$$\chi^{ijk}_{BQS} = \frac{\partial^{i+j+k}(P/T^4)}{\partial^i(\mu_B/T)\partial^j(\mu_Q/T)\partial^k(\mu_S/T)}, \tag{8}$$

where the pressure P is obtained from

$$P = \frac{T}{V}\ln Z. \tag{9}$$

The above susceptibilities computed in a model can then be converted easily to moments for a comparison with the measured data. For example, the mean M and variance σ^2 of the conserved charge distribution have one-to-one correspondence with the first two orders of susceptibility of the respective charge c:

$$M_c = \langle N_c\rangle = VT^3\chi_c^1, \tag{10}$$

$$\sigma_c^2 = \langle (N_c - \langle N_c\rangle)^2\rangle = VT^3\chi_c^2, \tag{11}$$

with N_c being the observed net charge of type c in an event while $\langle N_c\rangle$ is the ensemble average. We have evaluated the susceptibilities within HRG and estimated the influence of the missing resonances to the extraction of freezeout parameters thereof. It has been found that scaled variances σ^2/M of net Q and net B are well described within the HRG framework, while higher moments such as skewness and kurtosis show discrepancies, particularly at lower energies [12,30,31]. These higher moments are also sensitive to nonideal corrections, such as incorporating repulsive and attractive interactions within the HRG framework [32–35]. Hence, in this study we stick to σ^2/M of net Q and B to ascertain the influence of the systematics of the hadron spectrum on the freezeout surface extracted from the data on conserved charge fluctuation.

On the experimental front, several uncertainties can creep into the measurement of conserved charge fluctuations. The acceptance cuts in transverse momentum and rapidity are among them [10]. Also, the neutral particles are not detected, which means net-proton fluctuations only act as an approximate proxy for net B [36]. Currently, there is a tension between the PHENIX [37] and STAR [38,39] measurements for net charge fluctuation. In this work, we have extracted the freezeout parameters for STAR data alone. We expect the dependence of the freezeout parameters on the uncertainties of the hadron spectrum to be similar for STAR and PHENIX data.

While a single unified freezeout picture (1CFO) provides a good qualitative description across a broad range of beam energies, recent studies have shown that a natural step beyond 1CFO would be to consider flavor hierarchy in freezeout (2CFO), based on various arguments such as flavor hierarchy in QCD thermodynamic quantities on the lattice [40], hadron-hadron cross sections [41,42], and melting of in-medium hadron masses [43]. We have analyzed the yield data in both the freezeout schemes: 1CFO and 2CFO. However, for the conserved charge fluctuation study, currently only data for the moments of net protons (proxy for net baryons) [38] and net charge [39] are available. The net B and net Q fluctuations are dominated by the nonstrange sector, as the lightest hadrons contributing to these quantities are nonstrange. Thus, the analysis of the data on the conserved charge fluctuations is not sensitive to the thermal state of the strange sector. Hence, we have analyzed the data on higher moments of the conserved charges only within 1CFO.

III. HADRON SPECTRUM

We have performed our analysis with two different hadron spectra: the first set consists of only the confirmed hadrons and resonances from the PDG 2016 Review [5]. This includes all the mesons listed in the Meson Summary Table [5] that are marked confirmed and all baryons in the Baryon Summary

TABLE I. List of additional resonances in PDG-2016+ that are not included in PDG-2016. This consists of one- and two-star status baryons and unmarked mesons from PDG-2016 [5] that are yet to be confirmed experimentally.

Mesons		Baryons	
$h_1(1380)$	$f_2(1430)$	$N(1860)$	$N(1880)$
$f_1(1510)$	$f_2(1565)$	$N(1895)$	$N(1895)$
$\rho(1570)$	$h_1(1595)$	$N(2000)$	$N(2040)$
$a_1(1640)$	$f_2(1640)$	$N(2060)$	$N(2100)$
$a_2(1700)$	$\eta(1760)$	$N(2120)$	$N(2300)$
$f_2(1810)$	$a_1(1420)$	$N(2570)$	$N(2700)$
$\eta_2(1870)$	$\rho(1900)$	$\Delta(1750)$	$\Delta(1900)$
$f_2(1910)$	$a_0(1950)$	$\Delta(1940)$	$\Delta(2000)$
$\rho_3(1990)$	$f_0(2020)$	$\Delta(2150)$	$\Delta(2200)$
$\pi_2(2100)$	$f_0(2100)$	$\Delta(2300)$	$\Delta(2350)$
$f_2(2150)$	$\rho(2150)$	$\Delta(2390)$	$\Delta(2400)$
$f_0(2200)$	$f_4(2220)$	$\Delta(2750)$	$\Delta(2950)$
$\eta(2225)$	$\rho_3(2250)$		
$f_4(2300)$	$f_0(2330)$		
$\rho_5(2350)$	$a_6(2450)$		
$f_6(2510)$			
$K(1460)$	$K_2(1580)$	$\Lambda(1710)$	$\Lambda(2000)$
$K(1630)$	$K_1(1650)$	$\Lambda(2020)$	$\Lambda(2050)$
$K(1830)$	$K_0^*(1950)$	$\Lambda(2325)$	$\Lambda(2585)$
$K_2^*(1980)$	$K_2(2250)$	$\Sigma(1480)$	$\Sigma(1560)$
$K_3(2320)$	$K_5^*(2380)$	$\Sigma(1580)$	$\Sigma(1620)$
$K_4(2500)$	$K(3100)$	$\Sigma(1690)$	$\Sigma(1730)$
		$\Sigma(1770)$	$\Sigma(1840)$
		$\Sigma(1880)$	$\Sigma(1900)$
		$\Sigma(1940)$	$\Sigma(2000)$
		$\Sigma(2070)$	$\Sigma(2080)$
		$\Sigma(2100)$	$\Sigma(2455)$
		$\Sigma(2620)$	$\Sigma(3000)$
		$\Sigma(3170)$	$\Xi(1620)$
		$\Xi(2120)$	$\Xi(2250)$
		$\Xi(2370)$	$\Xi(2500)$
		$\Omega(2380)$	$\Omega(2470)$

Table [5] with three- or four-star status that are considered established. This we refer to as PDG-2016. The second set includes all the resonances from PDG-2016 as well as the other unmarked mesons from the Meson Summary Table and baryons from the Baryon Summary Table with one- or two-star status that await confirmation. This set is referred to as PDG-2016+. We have listed all the additional resonances in PDG-2016+ in Table I. We consider resonances with only up, down, and strange flavor valence quarks. It has been shown that the PDG-2016+ provides a satisfactory description in the hadronic phase of continuum lattice estimates of most thermodynamic quantities [17].

As emphasised earlier, BRs for unstable resonances are an important ingredient to compute the total hadron yields. While the PDG provides the BRs for most of the confirmed resonances, those for the unconfirmed resonances are missing. Hence, we have to make an assumption of their

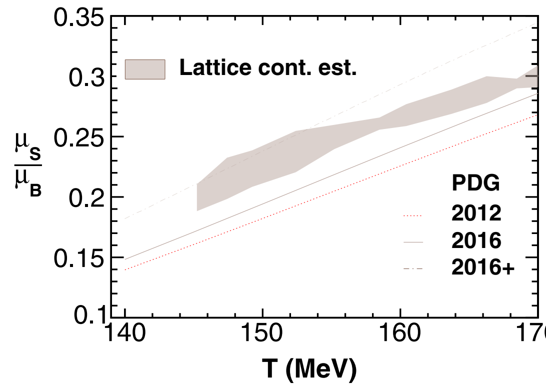

FIG. 1. Leading order μ_S/μ_B from a continuum estimate of the lattice [16] compared to that of HRG with hadron spectra from PDG-2012, -2016, and -2016+.

decay properties. The resonances of the same family have similar decay properties. Here, we assign to an unknown resonance R the decay properties of the known resonances with same quantum numbers as R and immediate to R in mass. For a systematic dependence on these unknown BRs, we perform our analysis with BRs taken from different resonances that are lighter as well as heavier to R. This systematic variation results in large variation in χ^2 and larger error bars in the fits with the PDG-2016+ spectrum as compared to PDG-2016. This also restricts us from including further unknown states predicted by theoretical studies, as the systematic uncertainties will be too large to draw any physics conclusions.

The μ_S extracted from the strangeness neutrality condition in Eq. (6) is sensitive to the strange hadron spectrum [16]. There have been studies on the lattice of the ratio μ_S/μ_B that constrain the hadron spectrum, specifically the strange sector [16,17]. It has been shown that the PDG-2012 hadron spectrum underestimates the ratio μ_S/μ_B at a given T. This can be addressed by including more states that are yet to be confirmed experimentally but predicted by quark-model-based studies or studies on the lattice. PDG-2016 has confirmed several new resonances while having others in the list of unconfirmed. We have analyzed their influence on this ratio by computing the same in PDG-2012, PDG-2016, and PDG-2016+. The ratio rises as we go from PDG-2012 to -2016 to -2016+, underlining the significance of these new resonances. This is particularly important to address the important issue of flavor hierarchy. As argued in Ref. [16], the same value of μ_S/μ_B is realiZed at a lower T on the lattice as well as in HRG with additional resonances apart from those listed in the 2012 version of PDG (PDG-2012) [44]. This brings down the strange freezeout T that can possibly modify the flavor hierarchy seen in the earlier 2CFO HRG fit with PDG-2012 [41]. We see in Fig. 1 that the results for PDG-2016 and -2016+ flank the continuum estimate of lattice. Thus, the PDG-2016+ cures the incorrect estimate of μ_S by PDG-2012 that lowers the freezeout T extracted for the strange sector. This makes it interesting to check the status of flavor hierarchy with PDG-2016+.

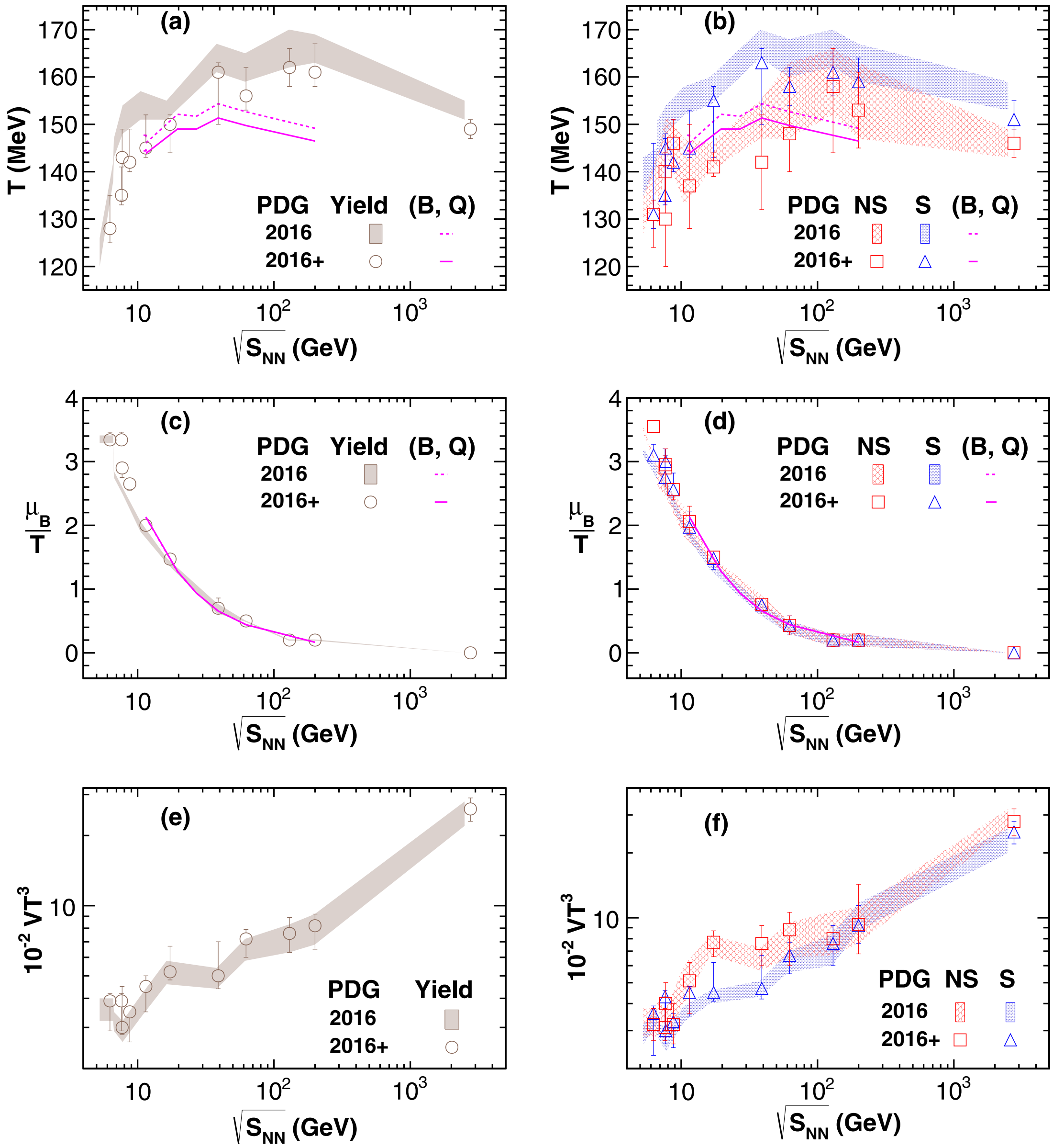

FIG. 2. The extracted thermal parameters in 1CFO (left) and 2CFO (right) schemes with PDG-2016 and PDG-2016+ hadron spectra. (B,Q) refer to the use of data on conserved charges net B and net Q to extract freezeout parameters.

IV. RESULTS

We have extracted the freezeout parameters from the data on mean mid-rapidity hadron yields [45–66] as well as scaled variance of net B and net Q [38,39]. The thermal parameters extracted from the 1CFO (left) and 2CFO (right) schemes are shown in Fig. 2. In the top panels, the extracted T has been plotted for different beam energies. We find that in 1CFO, as well as nonstrange and strange freezeout temperatures in 2CFO, the extracted temperatures seem to lower as we include more resonances. However, the large systematic uncertainties do not allow us to make a conclusive statement. Hence, we have also performed the fits to the data of conserved charge fluctuation, which are shown in dashed and solid lines in pink for PDG-2016 and PDG-2016+ respectively. The T extracted from the conserved charge fluctuation data clearly reveals the signature of cooling on addition of more resonances. As has been observed earlier [12], the T obtained from a fit to data on higher moments seem to be lower than that obtained from yields. The tension between these temperatures is bit lessened for $\sqrt{s_{NN}} < 20$ GeV. In 2CFO, the T extracted from fluctuation data for B and Q (which is dominated by the nonstrange sector as both the lightest charged hadron π and baryon p are nonstrange hadrons) is clearly closer to the nonstrange T for PDG-2016 as well as PDG-2016+.

In the middle panels we have plotted freezeout μ_B/T at different $\sqrt{s_{NN}}$. This baryon fugacity parameter seems to be quite stable across freezeout schemes, experimental data of yields and conserved charge fluctuation, as well as the different hadron spectrum. For $\sqrt{s_{NN}} < 10$ GeV, in a highly baryonic

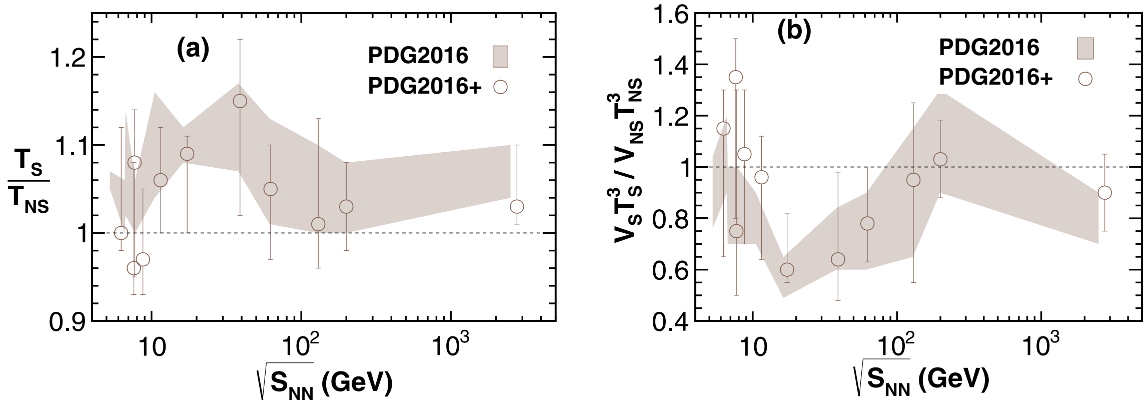

FIG. 3. Flavor hierarchy in freezeout T (left) and VT^3 (right) and its dependence on the hadron spectrum.

fireball, there seems to be a mild dependence on flavor as well as the hadron spectrum. Finally, the phase space volume factor VT^3, where V is the coordinate space freezeout volume, has been plotted in the bottom panels. This parameter also seems quite stable against addition of extra resonances in PDG-2016+. However, unlike μ_B/T this has a clear flavor hierarchy structure similar to T. The nonstrange phase space volume comes out to be larger than that of the strange phase space volume mostly.

There are correlations between the strange and nonstrange freezeout parameters. Hence, it might be misleading to comment on the flavor hierarchy from Fig. 2. Thus, we have extracted the strange to nonstrange freezeout parameters directly from the fits as well. These have been plotted in Fig. 3. We find that the flavor hierarchy in T obtained with PDG-2016 is same as that obtained earlier with PDG-2012 [41]. Further, for PDG-2016+, the central values clearly indicate the flavor hierarchy. The large error bars (due to the uncertainties coming from the systematic variation of the decay properties of the unconfirmed resonances) do not allow us to make a quantitative estimate of this hierarchy. However, even after including the error bars, qualitatively it is possible to state that data favor $T_s/T_{\rm ns} > 1$ while $V_s T_s^3/V_{\rm ns} T_{\rm ns}^3 < 1$ across most beam energies. At energies available at the CERN Large Hadron Collider (LHC), the addition of the extra resonances in PDG-2016+ seems to have eased the tension between the two flavors, as suggested by the central value of PDG-2016+ that falls outside the band of PDG-2016 and closer to unity. However, as was noted earlier with PDG-2012 [41], the discussion on flavor hierarchy, though triggered by the LHC data, seems most prominent in the range $\sqrt{s_{NN}} \sim$ 10–100 GeV. The qualitative nature of the flavor hierarchy structure remains in both the hadron spectra. The $T_s/T_{\rm ns}$ shows a broad peak-like structure while $V_s T_s^3/V_{\rm ns} T_{\rm ns}^3$ shows a trough in this range of beam energies. The central values seem to suggest a flip in the hierarchy for $\sqrt{s_{NN}} < 10$ GeV with PDG-2016+. However, again the systematic uncertainties are too large to make a conclusive statement on that. Such nonmonotonic behavior for $\sqrt{s_{NN}} \sim$ 10–100 GeV hints at possible delayed freezeout of the nonstrange sector [41]. It is to be noted that the beam energy scan data from STAR [67] show a very interesting trend in mean transverse mass $\langle m_T \rangle - m$, similar to VT^3 at these energies, whose origin is yet to be understood completely [68,69]. It would be interesting in the future to investigate whether these distinct trends in flavor hierarchy and transverse mass at these beam energies share a common physics origin.

Thus, we find that the systematics of the hadron spectrum mostly influence the freezeout T. The dimensionless parameters μ_B/T and VT^3 are comparatively more stable towards such systematics. The addition of more resonances mostly reduces T. This happens in two ways. First, with the addition of more strange resonances the required μ_S/μ_B from the strangeness neutrality condition shifts to lower T [16,17]. This cooling only occurs for the strange sector. The second way is through the feedown of these additional resonances. The feeddown to the nonstrange sector is from all resonances while that to the strange sector is only from the strange resonances. This would mean while the first factor cools only the strange T, the second factor cools both flavors, albeit more strongly the nonstrange T. This is the reason behind the survival of the flavor hierarchy on addition of the extra resonances.

We have, finally, plotted all the freezeout T and μ_B/T together in Fig. 4. The estimate of the QCD crossover transition from the hadron to the quark gluon plasma (QGP) phase from the lattice QCD approach is also shown for comparison by the two dashed lines. The dashed lines correspond to $T =$ 163 MeV (upper) and 145 MeV (lower) at $\mu_B = 0$ [70] and

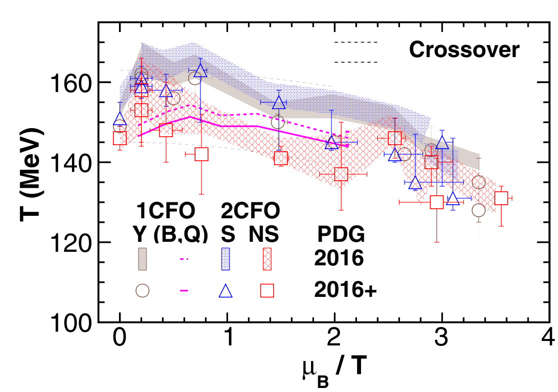

FIG. 4. T-μ_B/T plane: Freezeout coordinates in heavy ion collisions have been compared with the QCD crossover region as estimated in lattice QCD computations [70–74].

have curvatures ∼0.006 (upper) [71,72] and ∼0.01 (lower) [73,74] that cover estimates of the QCD crossover region from lattice QCD calculations. The PDG-2016 spectrum yields freezeout $T < 165$ MeV (central values). This results in a consistent picture between the hadronization surface estimated on the lattice and the freezeout temperature extracted. The addition of the suspected resonances in PDG-2016+ further shifts the freezeout surface into the hadron phase. Currently, lattice approaches can provide results up to $\mu_B/T \sim 2$. However, the freezeout parameters at lower beam energies that result in μ_B/T up to ∼4 suggest no abrupt change in curvature and probably a smooth continuation of the hadronization surface into higher baryon densities. It would be interesting to check how these results are modified on using a different variant of HRG where interhadron interactions are considered through attractive and repulsive channels [32–35].

V. SUMMARY

The analysis of the hadron yields within the hadron resonance gas framework provides an access to the freezeout surface. However such endeavors always suffer from the systematic uncertainties of the input hadron spectrum. The standard rule of thumb is to include all the confirmed resonances listed in the PDG. Studies of the hadron spectrum on the lattice as well as in quark models hint at the existence of many more resonances which are yet to be confirmed experimentally. Such missing resonances seem to have a considerable effect on thermodynamics and could also affect the phenomenology of freezeout in heavy ion collisions. In this work we have updated the thermal model fits with the latest PDG-2016 confirmed resonances listing as well as gauged the effect of those which are included in PDG-2016 but yet to be confirmed. The most significant effect is on the extracted temperature that drops by ∼5% while the other parameters such as the phase space volume VT^3 and baryon fugacity μ_B/T are almost insensitive to such changes in spectrum. These new freezeout temperatures with the updated hadron spectrum in both the freezeout schemes 1CFO and 2CFO are within the upper bound served by the lattice estimate of the hadronization temperature.

The drop in temperature is further confirmed by the analysis of the data on conserved charge fluctuation. The freezeout temperature extracted from the conserved charge fluctuation data is always smaller than that extracted from the data on mean hadron yields within 1CFO. However, the nonstrange freezeout temperature extracted within 2CFO from yield data is consistent with that extracted from scaled variance of net B and net Q data. The 2CFO scenario can be confirmed from the fluctuation data with the availability of data on higher moments of net S and its correlations with other flavors [75–78]. An obstacle in this regard is that Λ is currently not measured on an even-by-event basis and one has to rely on the data of only charged kaons [79]. At least at top STAR and LHC energies, when the fireball is dominantly mesonic, we expect the data on net kaon fluctuation to be a good proxy for net S [78].

Finally, one could ask how future updates on the hadron spectrum will influence our results. A comparison of the thermal fits for PDG-2016 and PDG-2016+ suggests that while the dimensionless parameters μ_B/T and VT^3 stay stable to such modifications of the hadron spectrum, the freezeout T is expected to fall further. The cooling happens primarily due to two factors:

(1) *The shift in μ_S/μ_B vs T plot towards lower T*. This shift is controlled by strange resonances. The newly added strange hadrons shift this plot further towards smaller T. In a 1CFO scenario where there is one freezeout T, this cools both strange and nonstrange sectors. Within a 2CFO scenario, this cools only the strange sector and reduces flavor hierarchy. As seen from Fig. 1, the PDG-2016+ spectrum already has a μ_S/μ_B vs T plot that is on the lower T edge of the continuum lattice estimate. This means future hadron spectrum updates that obey this lattice estimate cannot cool further through this mechanism. Since PDG-2016+ already favors a flavor hierarchy in freezeout parameters as seen in Fig. 3, we do not expect future updates on the hadron spectrum to diminish this hierarchy.

(2) *Feeddown from the additional resonances*. The feeddown from unstable additional resonances cools both nonstrange and strange sectors. However, while all resonances feed down to the nonstrange sector, only strange resonances feed to the strange sector. Thus, this feeddown mechanism is expected to cool the nonstrange sector more than the strange sector and hence enhance the current flavor hierarchy.

Thus, probably our study confirms that the data prefer a hierarchial treatment of flavors. However, 2CFO where the hierarchy is introduced in the thermodynamic state of the fireball is not the only way to introduce flavor dependence. It has been shown that one could also introduce flavor-dependent attractive and repulsive interactions [80]. It is important to construct observables to discriminate such scenarios of flavor hierarchy.

ACKNOWLEDGMENTS

S.C. acknowledges discussions and collaborations on freezeout with Rohini Godbole and Sourendu Gupta. S.C. is supported by the Polish Ministry of Science and Higher Education (MNiSW) and the National Science Centre Grant No. 2015/17/B/ST2/00101. B.M. acknowledges financial support from J.C. Bose Fellowship of DST, Govt. of India. S.S. acknowledges financial support from a DAE-SRC grant, Govt. of India.

[1] P. Braun-Munzinger, J. Stachel, J. P. Wessels, and N. Xu, Phys. Lett. B **365**, 1 (1996).
[2] G. D. Yen and M. I. Gorenstein, Phys. Rev. C **59**, 2788 (1999).
[3] J. Cleymans and K. Redlich, Phys. Rev. C **60**, 054908 (1999).

[4] F. Becattini, J. Cleymans, A. Keranen, E. Suhonen, and K. Redlich, Phys. Rev. C **64**, 024901 (2001).
[5] C. Patrignani *et al.* (Particle Data Group), Chin. Phys. C **40**, 100001 (2016).
[6] A. Andronic, P. Braun-Munzinger, and J. Stachel, Nucl. Phys. A **772**, 167 (2006).
[7] S. Chatterjee, S. Das, L. Kumar, D. Mishra, B. Mohanty, R. Sahoo, and N. Sharma, Adv. High Energy Phys. **2015**, 1 (2015).
[8] S. Chatterjee, A. K. Dash, and B. Mohanty, J. Phys. **G44**, 105106 (2017).
[9] F. Karsch and K. Redlich, Phys. Lett. B **695**, 136 (2011).
[10] P. Garg, D. K. Mishra, P. K. Netrakanti, B. Mohanty, A. K. Mohanty, B. K. Singh, and N. Xu, Phys. Lett. B **726**, 691 (2013).
[11] A. Bhattacharyya, S. Das, S. K. Ghosh, R. Ray, and S. Samanta, Phys. Rev. C **90**, 034909 (2014).
[12] P. Alba, W. Alberico, R. Bellwied, M. Bluhm, V. Mantovani Sarti, M. Nahrgang, and C. Ratti, Phys. Lett. B **738**, 305 (2014).
[13] S. Capstick and N. Isgur, Phys. Rev. D **34**, 2809 (1986); also published in *Hadron Spectroscopy - 1985*, April 1985, College Park, MD, edited by S. Oneda, *AIP Conf. Proc.* No. 132 (AIP, New York, 1985), p. 267.
[14] D. Ebert, R. N. Faustov, and V. O. Galkin, Phys. Rev. D **79**, 114029 (2009).
[15] R. G. Edwards, N. Mathur, D. G. Richards, and S. J. Wallace (Hadron Spectrum Collaboration), Phys. Rev. D **87**, 054506 (2013).
[16] A. Bazavov, H. T. Ding, P. Hegde, O. Kaczmarek, F. Karsch, E. Laermann, Y. Maezawa, S. Mukherjee, H. Ohno, P. Petreczky, C. Schmidt, S. Sharma, W. Soeldner, and M. Wagner, Phys. Rev. Lett. **113**, 072001 (2014).
[17] P. Alba *et al.*, Phys. Rev. D **96**, 034517 (2017).
[18] W. Broniowski and W. Florkowski, Phys. Lett. B **490**, 223 (2000).
[19] W. Broniowski, W. Florkowski, and L. Ya. Glozman, Phys. Rev. D **70**, 117503 (2004).
[20] J. Noronha-Hostler, C. Greiner, and I. A. Shovkovy, Phys. Rev. Lett. **100**, 252301 (2008).
[21] S. Chatterjee, R. M. Godbole, and S. Gupta, Phys. Rev. C **81**, 044907 (2010).
[22] P. M. Lo, M. Marczenko, K. Redlich, and C. Sasaki, Phys. Rev. C **92**, 055206 (2015).
[23] E. R. Arriola, W. Broniowski, E. Megias, and L. L. Salcedo, arXiv:1612.07091.
[24] J. Noronha-Hostler, arXiv:1612.07765.
[25] V. V. Begun, V. Yu. Vovchenko, and M. I. Gorenstein, arXiv:1701.03358.
[26] R. V. Gavai and S. Gupta, Phys. Lett. B **696**, 459 (2011).
[27] A. Bazavov, H. T. Ding, P. Hegde, O. Kaczmarek, F. Karsch, E. Laermann, S. Mukherjee, P. Petreczky, C. Schmidt, D. Smith, W. Soeldner, and M. Wagner, Phys. Rev. Lett. **109**, 192302 (2012).
[28] S. Borsanyi, Z. Fodor, S. D. Katz, S. Krieg, C. Ratti, and K. K. Szabo, Phys. Rev. Lett. **111**, 062005 (2013).
[29] A. Bazavov, H.-T. Ding, P. Hegde, O. Kaczmarek, F. Karsch, E. Laermann, S. Mukherjee, H. Ohno, P. Petreczky, C. Schmidt, S. Sharma, W. Soeldner, and M. Wagner, Phys. Rev. D **93**, 014512 (2016).
[30] S. Gupta, X. Luo, B. Mohanty, H. G. Ritter, and N. Xu, Science **332**, 1525 (2011).
[31] R. P. Adak, S. Das, S. K. Ghosh, R. Ray, and S. Samanta, Phys. Rev. C **96**, 014902 (2017).
[32] M. Albright, J. Kapusta, and C. Young, Phys. Rev. C **92**, 044904 (2015).
[33] V. Vovchenko, M. I. Gorenstein, and H. Stoecker, Phys. Rev. Lett. **118**, 182301 (2017).
[34] P. Huovinen and P. Petreczky, arXiv:1708.00879.
[35] V. Vovchenko, A. Pasztor, Z. Fodor, S. D. Katz, and H. Stoecker, Phys. Lett. B **775**, 71 (2017).
[36] M. Kitazawa and M. Asakawa, Phys. Rev. C **86**, 024904 (2012); **86**, 069902(E) (2012).
[37] A. Adare *et al.* (PHENIX Collaboration), Phys. Rev. C **93**, 011901 (2016).
[38] L. Adamczyk *et al.* (STAR Collaboration), Phys. Rev. Lett. **112**, 032302 (2014).
[39] L. Adamczyk *et al.* (STAR Collaboration), Phys. Rev. Lett. **113**, 092301 (2014).
[40] R. Bellwied, S. Borsanyi, Z. Fodor, S. D. Katz, and C. Ratti, Phys. Rev. Lett. **111**, 202302 (2013).
[41] S. Chatterjee, R. M. Godbole, and S. Gupta, Phys. Lett. B **727**, 554 (2013).
[42] K. A. Bugaev, D. R. Oliinychenko, J. Cleymans, A. I. Ivanytskyi, I. N. Mishustin, E. G. Nikonov, and V. V. Sagun, Europhys. Lett. **104**, 22002 (2013).
[43] J. M. Torres-Rincon, B. Sintes, and J. Aichelin, Phys. Rev. C **91**, 065206 (2015).
[44] J. Beringer *et al.* (Particle Data Group), Phys. Rev. D **86**, 010001 (2012).
[45] C. Alt *et al.* (NA49 Collaboration), Phys. Rev. C **77**, 024903 (2008).
[46] C. Alt *et al.* (NA49 Collaboration), arXiv:nucl-ex/0512033.
[47] C. Alt *et al.* (NA49 Collaboration), Phys. Rev. C **78**, 034918 (2008).
[48] C. Alt *et al.* (NA49 Collaboration), Phys. Rev. C **78**, 044907 (2008).
[49] S. V. Afanasiev *et al.* (NA49 Collaboration), Phys. Rev. C **66**, 054902 (2002).
[50] C. Alt *et al.* (NA49 Collaboration), Phys. Rev. C **73**, 044910 (2006).
[51] C. Alt *et al.* (NA49 Collaboration), Phys. Rev. Lett. **94**, 192301 (2005).
[52] S. Das (STAR Collaboration), Nucl. Phys. A **904-905**, 891c (2013).
[53] B. I. Abelev *et al.* (STAR Collaboration), Phys. Rev. C **79**, 034909 (2009).
[54] B. I. Abelev *et al.* (STAR Collaboration), Phys. Rev. C **79**, 064903 (2009).
[55] M. M. Aggarwal *et al.* (STAR Collaboration), Phys. Rev. C **83**, 024901 (2011).
[56] C. Adler *et al.* (STAR Collaboration), Phys. Rev. C **65**, 041901 (2002).
[57] J. Adams *et al.* (STAR Collaboration), Phys. Rev. Lett. **92**, 182301 (2004).
[58] K. Adcox *et al.* (PHENIX Collaboration), Phys. Rev. C **69**, 024904 (2004).
[59] K. Adcox *et al.* (PHENIX Collaboration), Phys. Rev. Lett. **89**, 092302 (2002).
[60] J. Adams *et al.* (STAR Collaboration), Phys. Lett. B **612**, 181 (2005).
[61] S. S. Adler *et al.* (PHENIX Collaboration), Phys. Rev. C **69**, 034909 (2004).

[62] J. Adams *et al.* (STAR Collaboration), Phys. Rev. Lett. **98**, 062301 (2007).

[63] B. Abelev *et al.* (ALICE Collaboration), Phys. Rev. C **88**, 044910 (2013).

[64] B. B. Abelev *et al.* (ALICE Collaboration), Phys. Rev. C **91**, 024609 (2015).

[65] B. B. Abelev *et al.* (ALICE Collaboration), Phys. Rev. Lett. **111**, 222301 (2013).

[66] B. B. Abelev *et al.* (ALICE Collaboration), Phys. Lett. B **728**, 216 (2014); **734**, 409(E) (2014).

[67] L. Adamczyk *et al.* (STAR Collaboration), Phys. Rev. C **96**, 044904 (2017).

[68] L. Van Hove, Phys. Lett. **118**, 138 (1982).

[69] B. Mohanty, Jan-e Alam, S. Sarkar, T. K. Nayak, and B. K. Nandi, Phys. Rev. C **68**, 021901 (2003).

[70] A. Bazavov, T. Bhattacharya, M. Cheng, C. DeTar, H. T. Ding, S. Gottlieb, R. Gupta, P. Hegde, U. M. Heller, F. Karsch, E. Laermann, L. Levkova, S. Mukherjee, P. Petreczky, C. Schmidt, R. A. Soltz, W. Soeldner, R. Sugar, D. Toussaint, W. Unger, and P. Vranas (HotQCD Collaboration), Phys. Rev. D **85**, 054503 (2012).

[71] O. Kaczmarek, F. Karsch, E. Laermann, C. Miao, S. Mukherjee, P. Petreczky, C. Schmidt, W. Soeldner, and W. Unger, Phys. Rev. D **83**, 014504 (2011).

[72] G. Endrodi, Z. Fodor, S. D. Katz, and K. K. Szabo, J. High Energy Phys. 04 (2011) 001.

[73] C. Bonati, M. D'Elia, M. Mariti, M. Mesiti, F. Negro, and F. Sanfilippo, Phys. Rev. D **92**, 054503 (2015).

[74] R. Bellwied, S. Borsanyi, Z. Fodor, J. Günther, S. D. Katz, C. Ratti, and K. K. Szabo, Phys. Lett. B **751**, 559 (2015).

[75] A. Chatterjee, S. Chatterjee, T. K. Nayak, and N. R. Sahoo, J. Phys. G **43**, 125103 (2016).

[76] J. Noronha-Hostler, R. Bellwied, J. Gunther, P. Parotto, A. Pasztor, I. P. Vazquez, and C. Ratti, arXiv:1607.02527.

[77] Z. Yang, X. Luo, and B. Mohanty, Phys. Rev. C **95**, 014914 (2017).

[78] C. Zhou, J. Xu, X. Luo, and F. Liu, Phys. Rev. C **96**, 014909 (2017).

[79] L. Adamczyk *et al.* (STAR Collaboration), arXiv:1709.00773.

[80] P. Alba, V. Vovchenko, M. I. Gorenstein, and H. Stoecker, arXiv:1606.06542.